# Power-Balanced Non-Orthogonal Multiple Access Based on Virtual Channel Optimization

Wenlong Xia, *Member, IEEE*, Yuanping Zhou, Guide Yang, and Ray T. Chen, *Fellow, IEEE*

***Abstract*—In this brief, we propose a virtual channel optimization method for downlink non-orthogonal multiple access (NOMA) systems. With this method, we show that superposed users' data can be separated successfully in power-balanced scenario for NOMA. We derive the optimum relative phase offset for two users as well as three users based on the minimum Euclidean distance (MED) among the superposed constellation points without channel state information at the transmitter (CSIT). We exploit maximum likelihood (ML) detector at the receiver as successive interference cancelation (SIC) is not applicable for power-balanced scenario. Since the complexity of ML is high, we design a low-complexity ML algorithm to substantially reduce the computational complexity. Simulation results for quadrature phase-shift keying (QPSK) modulation demonstrate the effectiveness and the performance of the proposed method.**

***Index Terms*—Minimum Euclidean distance, reduced complexity maximum likelihood, non-orthogonal multiple access, power balance, virtual channel.**

## I. Introduction

NON-ORTHOGONAL multiple access (NOMA) has been widely investigated to meet the requirements of the next generation mobile communications for extreme data rates increase, massive connections and low latency. By enabling multiple users to transmit their data at the same resources such as frequency, time and code domain, NOMA has shown its superiority over orthogonal multiple access (OMA) on spectral efficiency with affordable complexity [1], [2].

In general, NOMA can be implemented in power or code domain [2], [3]. We focus on the power domain NOMA in this brief. A distinguishing feature for power domain NOMA is that superposition coding in power domain is used at the transmitter and successive interference cancellation (SIC) is used at the receiver. The decoding performance of the SIC-based NOMA largely depends on the power differences among the users sharing the same resources. A strong user and a weak user have been suggested to be grouped together in a two-user NOMA scheme. Therefore, resource allocation and scheduling such as user grouping, fairness issues, power allocation, and decode ordering [4]–[6] have to be concerned due to the utilization of SIC. A NOMA for cellular future radio access is presented in [1], in which a tree-search based transmission power allocation (TTPA) is proposed. A joint user scheduling and power allocation for a downlink NOMA with imperfect CSI is investigated in [7]. Zhu *et al.* proposed max-min fairness and weighted sum rate optimization algorithm in [8]. In [9], round-Robin and proportional fairness (PF) scheduling are investigated to provide fast and effective scheduling. However, the computational complexity of the aforementioned scheduling algorithms is too high.

On the other hand, most of the existing scheduling algorithms assume the perfect or partial knowledge of channel state information at the transmitter (CSIT), which is impractical for some application scenarios such as unmanned aerial vehicle (UAV) communications [10], underwater acoustic (UWA) communications [11], and high-speed railway (HSR) communications [12]. In these cases, instantaneous channel gains are hardly stably obtained due to the rapidly changing channels or large feedback delay. It is modeled as a power-balanced situation in which a transmitter allocates equal power to different downlink users in the absence of CSIT in [10]. In addition, large channel differences among different users are crucial to guarantee the performance of conventional SIC. Nevertheless, grouping a strong user with a weak user is challenging in scenarios without comparable numbers of strong and weak users. To address this issue, a practical power balanced network-coded multiple access (NCMA) is proposed to group two weak users into a NOMA group in [13]. However, the computational complexity for NCMA is very high due to the joint use of physical-layer network coding (PNC) and multiuser decoding (MUD). Motivated by these demanding cases, we focus on the scenarios which CSIT is hard to obtain and try to reduce the complexity of NOMA implementation.

In this brief, we propose a low-complexity downlink NOMA scheme based on our previous work on virtual channel optimization [14]. With this virtual channel model, we optimize the phases of the users' signals for power-balanced scenario. In this case, it is very similar to the constellation rotation in [15], [16]. However, the optimal rotation angle without any CSIT is not well studied for constellation rotation. Moreover, the constellation rotation for 3 users under power-balanced scenario has not been reported to the best of our knowledge. In addition, the existing literatures on constellation rotation for NOMA assume maximum likelihood (ML) detector, which is of high computational complexity. To combat these challenges, we propose a reduced-complexity maximum likelihood (RML) method to recover users' data at the receiver based on an optimization criterion noted $\max(d_{min})$ by maximizing the minimum Euclidean distance (MED)

Manuscript received May 17, 2019; accepted June 21, 2019. Date of publication June 26, 2019; date of current version April 1, 2020. This work was supported by the China Scholarship Council under Grant 201706245027. This brief was recommended by Associate Editor I. W. H. Ho. *(Corresponding author: Wenlong Xia.)*

W. Xia, Y. Zhou, and G. Yang are with the School of Electronics and Information Engineering, Sichuan University, Chengdu 610065, China (e-mail: xwenlong@scu.edu.cn; ypzhou@scu.edu.cn; changkongck@163.com).

R. T. Chen is with the Electrical and Computer Engineering, University of Texas at Austin, Austin, TX 78758 USA (e-mail: chen@ece.utexas.edu).

Color versions of one or more of the figures in this paper are available online at http://ieeexplore.ieee.org.

Digital Object Identifier 10.1109/TCSII.2019.2925270

$d_{min}$ [17], [18]. The main contributions of this brief are two aspects: 1) we derive a close-form optimization equation for power-balanced NOMA without CSIT by maximizing the MED and obtain a fixed solution of the rotation angle for 2 users as well as 3 users. 2) We propose a low-complexity maximum likelihood detector to reduce the computational complexity without compromising the performance with quadrature phase shift keying (QPSK) modulation and validate the results by the numeric experiments.

## II. System Model

We consider a typical hybrid multiple access downlink NOMA, in which users are divided into different groups and NOMA is adopted among the users within a group, while OMA scheme is applied among the groups. BS is equipped with one antenna and simultaneously serves $K$ single-antenna user equipments (UEs) in a group. $K$ input data streams $s_k (k = 1, 2, \ldots, K)$, each going through a virtual channel $w_k = A_k e^{j\theta_k}$, where $A_k$ and $\theta_k$ are the amplitude and phase of $w_k$, respectively, are superposed and transmitted to $K$ users. Let $\boldsymbol{s} = [s_1, s_2, \ldots, s_K]^{\mathrm{T}}$ with $E[|s_k|^2] = 1$ and $\boldsymbol{w} = [w_1, w_2, \ldots, w_K]^T$ denote the users' data vector and the corresponding virtual channel vector, respectively. Thus, the superposed signal transmitted at the BS can be expressed as

$$x = \boldsymbol{w}^T \boldsymbol{s} = \sum_{k=1}^{K} w_k s_k \tag{1}$$

Then the received signal vector at the $k$th user can be given by

$$y_k = h_k x + z_k = h_k \sum_{k=1}^{K} w_k s_k + z_k \tag{2}$$

where $h_k$ and $z_k$ are the complex channel and noise at user $k$, respectively. We assume that all the channels are independent and identically distributed (i.i.d.) complex Gaussian vector with zero mean and unit variance. $z_k$ is the additive white Gaussian noise (AWGN) with zero mean and variance $\sigma_k^2$. For power-balanced situation such as cell-edge users or unmanned aerial vehicle in [10], it is infeasible to distribute power among different users in the absence of CSIT, so we set $A_k = 1$ for all users, and then (2) can be rewritten as

$$y_k = h_k \sum_{k=1}^{K} w_k s_k + z_k = h_k \sum_{k=1}^{K} e^{j\theta_k} s_k + z_k \tag{3}$$

We try to optimize the phase $\theta_k (k = 1, 2, \ldots, K)$ of the virtual channel under the criterion of maximizing the MED among the superposed symbols. For this power-balanced model, the superposed users' signals have the same power level and typical SIC cannot be used, we resort to the ML detector to decode the users' data. Apparently, the computational complexity of classical ML detector is high, so we design a two-step low-complexity ML to reduce the computational complexity as described in Section III-C. The structure of the proposed power-balanced NOMA based on virtual channel optimization is shown in Fig. 1.

## III. Power-Balanced NOMA

Conventional NOMA exploits the power difference to separate users and SIC is used to decode multiple users' signals.

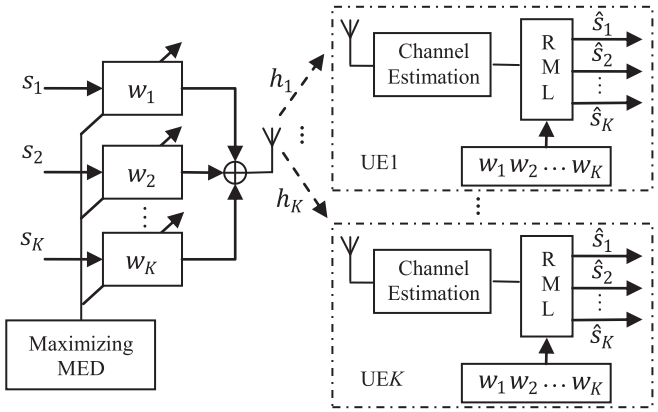


Fig. 1. The power-balanced NOMA with virtual channel optimization.

However, for power-balanced NOMA where two users are assigned the same power level, part of the points are overlapped and become indistinguishable [10, Fig. 6(a)]. We address this issue by adopting virtual channel optimization and maximizing the MED among the superposed points.

### A. Maximizing the Minimum Euclidean Distance

The ML detector relies on the Euclidean distance among the users' symbols at the receiver. Thus we can optimize the decoding performance by maximizing the minimum Euclidean distance. Let $\mathcal{C}$ denote the set of all transmitted users' symbols and $\mathcal{S}$ denote the finite set of all possible superposed vectors $\Xi$, then the squared MED $d_{min}^2$ of the received symbols at the $k$th receiver can be expressed as

$$d(k)_{min}^2 = \min_{\Xi_p, \Xi_q \in \mathcal{S}, \Xi_p \neq \Xi_q} \|h_k(\Xi_p - \Xi_q)\|^2 \tag{4}$$

where $\Xi_p = \sum_{k=1}^{K} w_k s_k(p_k)$, $\Xi_q = \sum_{k=1}^{K} w_k s_k(q_k)$. $s_k(p_k), s_k(q_k) \in \mathcal{C}$. Note that the channel coefficient $h_k$ is generally known to the receiver via channel estimation and only scales the MED. Then we can cancel the impact of $h_k$ at receiver side. Thereby, our proposed method can reduce the complexity since maximizing the MDE can be conducted among the vectors $\Xi$ and the CSIT is not necessary to be fed back to the transmitter. Furthermore, $\Xi_p$ and $\Xi_q$ are the function of $w_k, k \in \{1, \ldots, K\}$ which is determined by $\theta_k$, let us define $\Gamma_{min}(\boldsymbol{\theta})$ as

$$\Gamma_{min}(\boldsymbol{\theta}) = \min_{\Xi_p, \Xi_q \in \mathcal{S}, \Xi_p \neq \Xi_q} \|\Xi_p - \Xi_q\|^2 \tag{5}$$

where $\boldsymbol{\theta} = [\theta_1, \theta_2, \ldots, \theta_K]$, then the optimization problem of maximizing $d_{min}$ can be formulated as

$$\mathcal{W}_{opt}(\boldsymbol{\theta}) \triangleq max(\Gamma_{min}(\boldsymbol{\theta})) \tag{6}$$

We assume that the number of users in one NOMA group is 2 and QPSK constellation sets $\{\exp(\pm \mathrm{j}\pi/4), \exp(\pm \mathrm{j}3\pi/4)\}$ are used by two users. Since $h_k$ is known to the user $k$ via channel estimation, the squared distance $d_{pq}^2 = \|(\Xi_p - \Xi_q)\|^2$ for any two symbols $p$ and $q$ can be obtained from the normalized received superposed constellation as shown in Fig. 2. The 16 points labeled from "A" to "P" correspond to the superposed constellation symbols and "$E'$" represents the symbol before rotating. To maximize the squared MED $d_{min}^2$, the nearest neighbors should have the same distance [17, Appendix D].

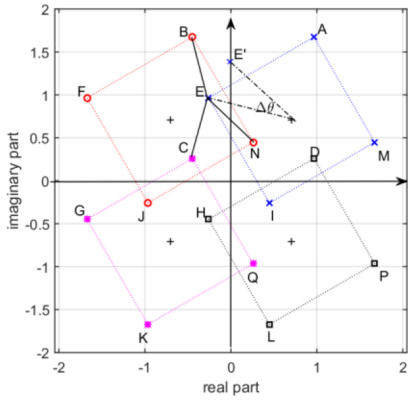


Fig. 2. Maximizing $d_{min}$ for normalized received superposed constellation.

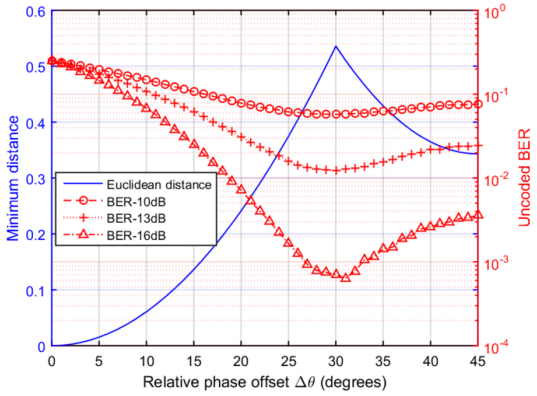


Fig. 3. The minimum distance and uncoded BER in terms of phase offset.

Then we have one optimal solution $d_{BE}^2 = d_{EC}^2 = d_{EN}^2$ due to the symmetry of the superposed constellation, where

$$d_{BE}^2 = \|(\Xi_B - \Xi_E)\|^2 = 4 - 4\cos(\Delta\theta) \quad (7)$$

$$d_{EC}^2 = \|(\Xi_E - \Xi_C)\|^2 = 6 - 4\cos(\Delta\theta) - 4\sin(\Delta\theta) \quad (8)$$

$$d_{EN}^2 = \|(\Xi_E - \Xi_N)\|^2 = 6 - 4\cos(\Delta\theta) - 4\sin(\Delta\theta) \quad (9)$$

Without loss of generality, $\Xi_B = e^{j\theta_1}(e^{j\frac{3\pi}{4}} + e^{j\Delta\theta}e^{j\frac{\pi}{4}})$, $\Xi_E = e^{j\theta_1}(e^{j\frac{\pi}{4}} + e^{j\Delta\theta}e^{j\frac{3\pi}{4}})$, $\Xi_C = e^{j\theta_1}(e^{-j\frac{3\pi}{4}} + e^{j\Delta\theta}e^{j\frac{\pi}{4}})$, $\Xi_N = e^{j\theta_1}(e^{j\frac{3\pi}{4}} + e^{j\Delta\theta}e^{-j\frac{\pi}{4}})$, respectively. $\Delta\theta = \theta_2 - \theta_1$ denotes one user's constellation rotation relative to the other.

Obviously, $d_{EC}^2 = d_{EN}^2$ always holds. For $d_{BE}^2 = d_{EC}^2$ using (7) and (8), we obtain $\sin(\Delta\theta) = 1/2$, i.e., $\Delta\theta = 30°$. Note that the maximum MED can be guaranteed when the angle difference is 30 degree regardless of the value of $\theta_1$. Then we can just set $\theta_1 = 0$ to simplify the implementation at the transmitter. In this way, user 1 and user 2 have a fixed phase difference, which can benefit the channel estimation for NOMA scheme.

Fig. 3 depicts the MED in terms of $\Delta\theta$, it can be seen that the maximum distance is obtained at $\Delta\theta = 30$ degree, which validate the analytical solution above. It also shows the uncoded BER performance for different SNR at 10dB, 13dB and 16dB, respectively. The optimal performance can be achieved when the phase offset $\Delta\theta = 30$ degree as well.

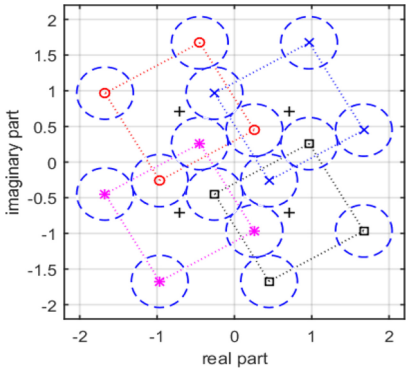


Fig. 4. Searching space for our reduced complexity ML detector.

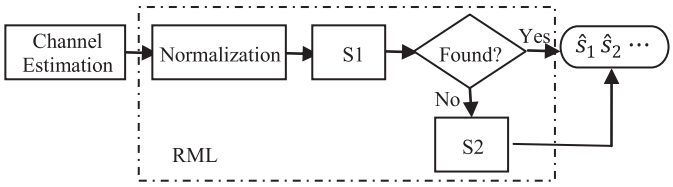


Fig. 5. The structure of two-step search for RML decoder.

### B. Reduced Complexity ML Detection Scheme

Once estimating the channel coefficient $h_k$, the normalized received symbol from (2) is given by

$$\hat{y}_k = x + \frac{z_k}{h_k} = \sum_{k=1}^{K} w_k s_k + \frac{z_k}{h_k} \quad (10)$$

This can be viewed as a degraded Gaussian broadcast channel [19] with noise variance $n_k$ at user $k$, where $n_k = \sigma_k^2/|h_k|^2$. For our setup, $x = s_1 + e^{j\Delta\theta}s_2$, from (7), the maximum minimum distance of two points $\check{d}_{min}^2 = 4 - 2\sqrt{3}$ at optimal $\Delta\theta = 30°$. This distance remains constant after cancelling the impact of $h_k$. Furthermore, the distances of nearest points for 12 points {B, C, D, E, G, H, I, J, L, M, N, Q} are equal due to the symmetry of the superposed constellation. Therefore, like the ML detection in spatial multiplexing systems [20], [21], the search radius for our scheme can be restricted to $\check{d}_{min}^2/4$ as shown in Fig. 4 thanking to the maximum minimum distance metric adopted. This can be represented by

$$\left|\hat{y}_k - \sum_{k=1}^{K} w_k s_k\right|^2 \leq \frac{\check{d}_{min}^2}{4} \quad (11)$$

It can be seen from Fig. 4 that this search radius does not cover the whole region. For simplicity, we use two steps search: searching the candidate points in the circle with radius of $\check{d}_{min}/2$ first (termed S1), if a valid point is found, and then stop searching, otherwise, using the exhaustive search to find the nearest point (termed S2). The structure of the two-step search is illustrated in Fig. 5. In this way, the computational complexity can be reduced because the search region is restricted to a smaller space and a point is successfully found at the very first step especially at high SNR.

### C. Power-Balanced NOMA Beyond Two Users

Now we consider one NOMA group with 3 user equipments (UEs) served simultaneously. Then (3) can

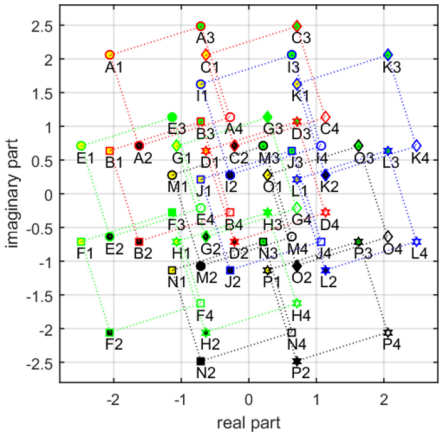


Fig. 6. Normalized superposed constellation for 3 users.

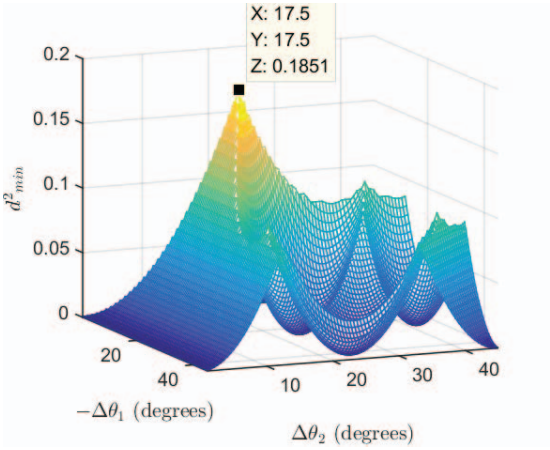


Fig. 7. The minimum squared distance for 3 users in terms of $\Delta\theta_1$ and $\Delta\theta_2$.

be rewritten as

$$y_k = h_k\left(e^{j\theta_1}s_1 + e^{j\theta_2}s_2 + e^{j\theta_3}s_3\right) + z_k$$
$$= h_k e^{j\theta_2}\left(e^{j\Delta\theta_1}s_1 + s_2 + e^{j\Delta\theta_2}s_3\right) + z_k \quad (12)$$

where $\Delta\theta_1 = \theta_1 - \theta_2$ and $\Delta\theta_2 = \theta_3 - \theta_2$. The superposed constellation for 3 users is illustrated in Fig. 6.

Appling the same method in Section III-B, the nearest neighbors should have the same distance to maximize $d^2_{min}$, i.e., $d^2_{\text{J1D1}} = d^2_{\text{J1M1}} = d^2_{\text{J1E4}} = d^2_{\text{J1I2}}$, we have

$$d^2_{\text{J1M1}} = \|(\Xi_{\text{J1}} - \Xi_{\text{M1}})\|^2 = 4 - 4\cos(\Delta\theta_1) \quad (13)$$
$$d^2_{\text{J1D1}} = \|(\Xi_{\text{J1}} - \Xi_{\text{D1}})\|^2 = 4 - 4\cos(\Delta\theta_1) \quad (14)$$
$$d^2_{\text{J1E4}} = \|(\Xi_{\text{J1}} - \Xi_{\text{E4}})\|^2 = [2\sin\gamma\cos\left(\varphi - \frac{\pi}{4}\right)]^2 + [2\cos\gamma\cos\left(\varphi - \frac{\pi}{4}\right) - \sqrt{2}]^2 \quad (15)$$
$$d^2_{\text{J1I2}} = \|(\Xi_{\text{J1}} - \Xi_{\text{I2}})\|^2 = 4 - 4\cos(\Delta\theta_2) \quad (16)$$

where $\Xi_{\text{J1}} = e^{j\theta_2}(e^{j\Delta\theta_1}e^{j\frac{\pi}{4}} + e^{-j\frac{3\pi}{4}} + e^{j\Delta\theta_2}e^{j\frac{3\pi}{4}})$, $\Xi_{\text{M1}} = e^{j\theta_2}(e^{j\Delta\theta_1}e^{-j\frac{\pi}{4}} + e^{j\frac{3\pi}{4}} + e^{j\Delta\theta_2}e^{j\frac{3\pi}{4}})$, $\Xi_{\text{D1}} = e^{j\theta_2}(e^{j\Delta\theta_1}e^{j\frac{3\pi}{4}} + e^{-j\frac{\pi}{4}} + e^{j\Delta\theta_2}e^{j\frac{3\pi}{4}})$, $\Xi_{\text{E4}} = e^{j\theta_2}(e^{j\Delta\theta_1}e^{-j\frac{3\pi}{4}} + e^{j\frac{3\pi}{4}} + e^{j\Delta\theta_2}e^{-j\frac{\pi}{4}})$, $\Xi_{\text{I2}} = e^{j\theta_2}(e^{j\Delta\theta_1}e^{j\frac{\pi}{4}} + e^{j\frac{3\pi}{4}} + e^{j\Delta\theta_2}e^{-j\frac{3\pi}{4}})$, $\gamma = \frac{\Delta\theta_1+\Delta\theta_2}{2}$, $\varphi = \frac{\Delta\theta_1-\Delta\theta_2}{2}$, respectively. From (13) and (14), $d^2_{\text{J1D1}} = d^2_{\text{J1M1}}$ always holds. From (14) and (16), we have $\Delta\theta_2 = -\Delta\theta_1$. By applying this solution to (15) and solving (15) and (16) jointly, we obtain $\Delta\theta_2 = -\Delta\theta_1 = 17.53$ degree.

The solution is independent of $\theta_2$. For simplicity, we set $\theta_2 = 0$. Fig. 7 presents the MED in terms of $\Delta\theta_1$ and $\Delta\theta_2$ in steps of 0.5 degree. The maximum distance is achieved at $\Delta\theta_2 = -\Delta\theta_1 = 17.5$ degree. And the normalized maximum MED is 0.185. This validates the solution above for 3 users.

## IV. Numerical Results

In this section, we will demonstrate the performance of our proposed virtual channel scheme with the existing schemes. The transmitted symbols for user 1 and user 2 are belong to the following power normalized QPSK constellation set: $\mathcal{C} = \{\exp(\pm j\pi/4), \exp(\pm j3\pi/4)\}$. We assume AWGN channels and a convolutional code with polynomials $[133, 171]_8$ of rate-1/2 [22] used by two users. To compare with NCMA approach, which is also proposed for power-balanced application, we employ the same packet setting as described in [10]. For

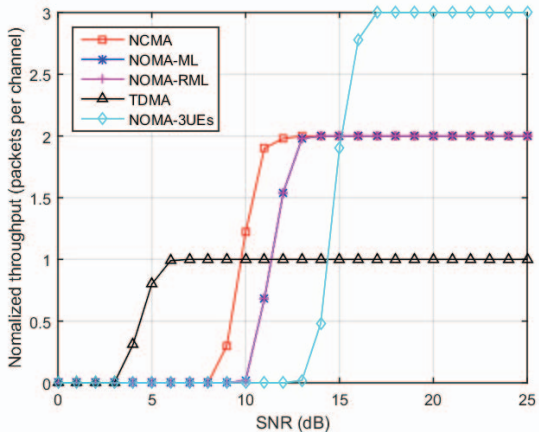


Fig. 8. Overall normalized throughputs comparison.

packet decoding, our scheme exploits RML to separate users and then adopts viterbi decoder as channel decoding, while NCMA exploits the maximum a posteriori (MAP) algorithm to separate two users and viterbi decoder is adopted as channel decoding as well.

Fig. 8 shows the normalized throughputs for NCMA, NOMA-ML, NOMA-RML and TDMA. It can be seen that NCMA and NOMA outperform TDMA due to concurrent transmissions of two users or three users (NOMA-3UEs). NOMA with ML and NOMA with RML have the same performance but much lesser computational complexity for the latter. NCMA has slight improvement than NOMA while the computational complexity is much higher than that of our proposed scheme. Fig. 9 demonstrates the normalized execution time ($\frac{T_X}{T_{TDMA}}$) for three schemes and 3UEs as well at 7dB, 12dB and 17dB with respect to the number of packets taking TDMA as a benchmark, where $T_X$ and $T_{TDMA}$ denote the execution time (including multiuser separation and channel decoding) to decode one packet for $X$ ($X \in$ {NCMA, NOMA-ML, NOMA-RML, NOMA-3UEs}) and TDMA schemes, respectively. These schemes are implemented on a Dell Inspiron 7559 with Intel i7-6700HQ CPU@2.60 GHz and 8GB RAM using MATLAB without any optimization. It can be seen that NCMA has the highest computational complexity. The normalized time for NCMA and NOMA-ML does not vary with SNR, whereas that of NOMA-RML varies with SNR due to

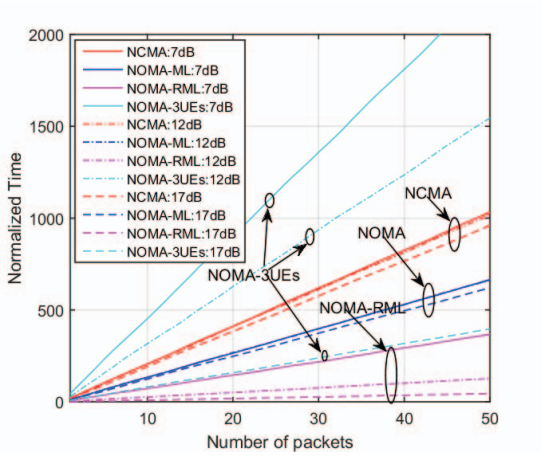


Fig. 9. Normalized time comparison in terms of the number of packets at SNR = 7dB, 12dB and 17dB.

the two steps search scheme adopted. In Fig. 9, NOMA-RML presents much lesser complexity especially at high SNR. The average cost reduction ratio of NOMA-RML versus NCMA at 17dB is $\eta = (T_{NCMA} - T_{NOMA-RML})/T_{NCMA} = 0.957$. This indicates that our proposed scheme substantially reduces the complexity of decoding compared to NCMA at high SNR. For 3 users' scenario, the number of superposed points is 64, which is fourfold greater than that of 2 users, so the computational cost is also four times higher as compared that of 2 users. However, RML method can still dramatically reduce the complexity at high SNR as can be seen in Fig. 9 for NOMA-3UEs at 17dB. At low SNR, most of the searches fall into the second step which is the conventional ML algorithm, so the computational cost is almost four times higher than that of 2 users' case.

Noted that our method works well for QPSK, and it might be applied to $M$-PSK as well such as 8PSK which can be found in [15, Sec. III-B], where $M = 2^{\lambda}$, $\lambda$ being a positive integer. But for high order $M$-QAM modulation such as 16QAM, the performance might show little improvement due to the high density of constellation points and needs further investigation.

## V. Conclusion

In this brief, a power-balanced NOMA scheme based on virtual channel optimization is proposed. By maximizing the minimum Euclidean distance of superposed symbols at the transmitter, users' data can be successfully decoded using the reduced complexity ML detector without CSIT. The theoretical relative phase offset is derived and the performance is verified by experimental simulation for 2 and 3 users. This brief can substantially reduce the overall complexity since the knowledge of channel information is dispensable at transmitter and a low-complexity decoding algorithm is exploited. It provides a better way to balance the tradeoff between performance and complexity. Our scheme can extend the NOMA application to more complicate scenarios such as HSR and UAV in which the robust channel state information is particularly challenging to obtain. Furthermore, our proposed scheme can pair two or more cell-edge (weak) users into a NOMA group and thus boost the overall system throughput of NOMA.

## References

[1] Y. Saito, Y. Kishiyama, A. Benjebbour, T. Nakamura, A. Li, and K. Higuchi, "Non-orthogonal multiple access (NOMA) for cellular future radio access," in *Proc. IEEE VTC Spring*, Dresden, Germany, Jun. 2013, pp. 1–5.

[2] S. M. R. Islam, N. Avazov, O. A. Dobre, and K.-S. Kwak, "Power-domain non-orthogonal multiple access (NOMA) in 5G systems: Potentials and challenges," *IEEE Commun. Surveys Tuts.*, vol. 19, no. 2, pp. 721–742, 2nd Quart. 2017.

[3] L. Dai, B. Wang, Y. Yuan, S. Han, I. C. Lin, and Z. Wang, "Non-orthogonal multiple access for 5G: Solutions, challenges, opportunities, and future research trends," *IEEE Commun. Mag.*, vol. 53, no. 9, pp. 74–81, Sep. 2015.

[4] S.Timotheou and I. Krikidis, "Fairness for non-orthogonal multiple access in 5G systems," *IEEE Signal Process. Lett.*, vol. 22, no. 10, pp. 1647–1651, Oct. 2015.

[5] M. D. S. Ali, H. Tabassum, and E. Hossain, "Dynamic user clustering and power allocation for uplink and downlink non-orthogonal multiple access (NOMA) systems," *IEEE Access*, vol. 4, pp. 6325–6343, 2016.

[6] Y.-R. Tsai and H.-A. Wei, "Quality-balanced user clustering schemes for non-orthogonal multiple access systems," *IEEE Commun. Lett.*, vol. 22, no. 1, pp. 113–116, Jan. 2018.

[7] F. Fang, H. Zhang, J. Cheng, S. Roy, and V. C. M. Leung, "Joint user scheduling and power allocation optimization for energy-efficient NOMA systems with imperfect CSI," *IEEE J. Sel. Areas Commun.*, vol. 35, no. 12, pp. 2874–2885, Dec. 2017.

[8] J. Zhu, J. Wang, Y. Huang, S. He, X. You, and L. Yang, "On optimal power allocation for downlink non-orthogonal multiple access systems," *IEEE J. Sel. Areas Commun.*, vol. 35, no. 12, pp. 2744–2757, Dec. 2017.

[9] J. He, Z. Tang, Z. Tang, H.-H. Chen, and C. Ling, "Design and optimization of scheduling and non-orthogonal multiple access algorithms with imperfect channel state information," *IEEE Trans. Veh. Technol.*, vol. 67, no. 11, pp. 10800–10814, Nov. 2018.

[10] H. Pan, S. C. Liew, J. Liang, Y. Shao, and L. Lu, "Network-coded multiple access on unmanned aerial vehicle," *IEEE J. Sel. Areas Commun.*, vol. 36, no. 9, pp. 2071–2086, Sep. 2018.

[11] L. Ma, S. Zhou, G. Qiao, S. Liu, and F. Zhou, "Superposition coding for downlink underwater acoustic OFDM," *IEEE J. Ocean. Eng.*, vol. 42, no. 1, pp. 175–187, Jan. 2017.

[12] X. Ren, M. Tao, and W. Chen, "Compressed channel estimation with position-based ICI elimination for high-mobility SIMO-OFDM systems," *IEEE Trans. Veh. Technol.*, vol. 65, no. 8, pp. 6204–6216, Aug. 2016.

[13] H. Pan, L. Lu, and S. C. Liew, "Practical power-balanced non-orthogonal multiple access," *IEEE J. Sel. Areas Commun.*, vol. 35, no. 10, pp. 2312–2327, Oct. 2017.

[14] G. Yang, Y. Zhou, and W. Xia, "Virtual channel optimization for overloaded MIMO systems," *IEEE Trans. Circuits Syst. II, Exp. Briefs*, vol. 65, no. 3, pp. 331–335, Mar. 2018.

[15] S. Kundu and B. S. Rajan, "Adaptive constellation rotation scheme for two-user fading MAC with quantized fade state feedback," *IEEE Trans. Wireless Commun.*, vol. 12, no. 3, pp. 1073–1083, Mar. 2013.

[16] M. J. Hagh and M. R. Soleymani, "Constellation rotation for DVB multiple access channels with raptor coding," *IEEE Trans. Broadcast.*, vol. 59, no. 2, pp. 290–297, Jun. 2013.

[17] L. Collin, O. Berder, P. Rostaing, and G. Burel, "Optimal minimum distance-based precoder for MIMO spatial multiplexing systems," *IEEE Trans. Signal Process.*, vol. 52, no. 3, pp. 617–627, Mar. 2004.

[18] X. Xu and Z. Chen, "Recursive construction of minimum Euclidean distance-based precoder for arbitrary-dimensional MIMO systems," *IEEE Trans. Commun.*, vol. 62, no. 4, pp. 1258–1271, Apr. 2014.

[19] L. Li and A. J. Goldsmith, "Capacity and optimal resource allocation for fading broadcast channels. I. Ergodic capacity," *IEEE Trans. Inf. Theory*, vol. 47, no. 3, pp. 1083–1102, Mar. 2001.

[20] J.-S. Kim, S.-H. Moon, and I. Lee, "A new reduced complexity ML detection scheme for MIMO systems," *IEEE Trans. Commun.*, vol. 58, no. 4, pp. 1302–1310, Apr. 2010.

[21] X. Dai, S. Sun, and Y. Wang, "Reduced-complexity performance-lossless (quasi-)maximum-likelihood detectors for S-QAM modulated MIMO systems," *Electron. Lett.*, vol. 49, no. 11, pp. 724–725, May 2013.

[22] *IEEE Standard for Information Technology—Telecommunications and Information Exchange Between Systems Local and Metropolitan Area Networks—Specific Requirements—Part 11: Wireless LAN Medium Access Control (MAC) and Physical Layer (PHY) Specifications Amendment 4: Enhancements for Very High Throughput for Operation in Bands Below 6 GHz*, IEEE Standard 802.11ac, 2013.